Supplement of

Sea spray promotes the sea-to-air transfer of dissolved organic carbon during phytoplankton bloom

Jie Hu[1], Jianlong Li[1], Narcisse Tsona Tchinda[1], Christian George[2, 3], Feng Xu[4], Min Hu[4], and Lin Du[1, 2, 5, *]

[1]Qingdao Key Laboratory for Prevention and Control of Atmospheric Pollution in Coastal Cities, Environment Research Institute, Shandong University, Qingdao 266237, China

[2]School of Environmental Science and Engineering, Shandong University, Qingdao 266237, China

[3]Universite Claude Bernard Lyon 1, CNRS, IRCELYON, UMR 5256, Villeurbanne F-69100, France

[4]State Key Laboratory of Regional Environment and Sustainability, International Joint Research Center for Atmospheric Research (IJRC), College of Environmental Sciences and Engineering, Peking University, Beijing 100871, China

[5]State Key Laboratory of Microbial Technology, Shandong University, Qingdao 266237, China

Corresponding to: Lin Du (lindu@sdu.edu.cn)

S1. Generation of nascent SSA

The main body of SSA simulation is made of transparent acrylic plastic with a volume of 180 L (length × width × height = 0.6 × 0.5 × 0.6 m^3). An overflow pipe with a slit (length × width = 20 cm × 2 mm) spans the upper space of the tank. As the centrifugal pump is running, seawater at the bottom of the tank is continuously pumped into the overflow pipe at a flow rate of 20 L min^{-1}, and after passing through the slit, a plunging waterfall is formed to hit the seawater surface to generate nascent SSA. Purified zero air (Zero Air Supply, Model 111, Thermo Scientific) enters as carrier air for the nascent SSA through the air inlet at the top of the tank and exits through the air outlet. A T-joint was set up at the air outlet to regulate fluctuations in the air flow rate between the air supply system and the sampling system. SSA sample airflow was dried by a diffusion drying tube (MD700-12F-3, Perma Pure, USA) to eliminate the effect of humidity on the SSA diameter (relative humidity <30%). Considering the effect of seawater temperature on SSA formation and composition (Hu et al., 2024), all experiments were conducted at a constant temperature of 25 ℃.

S2. Collection of nascent SSA

A single particle sampler (DKL-2, Genstar electronic technology Co., Ltd., China) with carbon coated copper grids (T11023, Tianld Co., Ltd., China) was used to collect SSA single particles at a flow rate of 1 L min^{-1} for 30 min. The copper grids were stored in a dry environment at -20 ℃ until analyzed by transmission electron microscopy (TEM, FEI Tecnai G2 F20, Thermo Fisher Scientific, USA). After that, SSA was sampled on a low-pressure cascade impactor (DLPI+, Dekati Ltd., Finland) with a flow rate of 10 L min^{-1} for 10 h. SSA was classified into 14 stages by aerodynamic cutoff diameter within the range of 0.016-10 μm (Table S2) and collected at each stage using a quartz fiber filter (25 mm, QMA, Whatman) which was pre-baked at 550 ℃ for 6 h. These filters were divided into two fractions: a submicron sample (0.016-0.94 μm) and a supermicron sample (1.62-10 μm). Each fraction was extracted with 10 mL ultrapure water (>18.2 MΩ·cm, 25 ℃, Millipore) with ultrasound assistance for 30 min, and the extraction was filtered with 0.45 μm filter. Procedure blanks were prepared by blank quartz fiber filters with the same treatment as SSA samples.

S3. Preparation of samples and instrumental conditions for ultra-high resolution mass spectrometry

The Bond Elut PPL (Priority Pollutant) solid-phase extraction column (100 mg/3 mL, Agilent Technologies) was first activated by passing three column volumes of chromatography-grade methanol through it. Next, the packing material was rinsed with three column volumes of acidified ultrapure water (HCl = 0.01 M, pH = 2). The sample was then passed through the column at a flow rate of approximately 1 mL/min. Afterward, the packing was completely dried with high-purity nitrogen.

The adsorbed organics were slowly eluted from the packing using chromatography-grade methanol. The eluate was evaporated to dryness with high-purity nitrogen and subsequently re-dissolved in a 300 μL solution (v/v = 1:1) of methanol and ultrapure water for further analysis.

Organics were separated using a C18 column (Waters, Atlantis^{TM} T3 3 μm, 2.1×150 mm). Ultrapure water (eluent A) containing 0.1% (v/v) formic acid and acetonitrile (eluent B) were used as mobile phases at a flow rate of 0.3 mL/min. The gradient elution conditions are shown in Table S4. The settings for the mass spectrometry section were as follows: source type was ESI-, capillary temperature was 275 ℃, sheath gas flow was 20 psi, aux gas flow was 5 psi, and source voltage was 4.20 kV.

S4. Parameters used to characterize the molecular formulas in the different samples

The m/z signals from the corresponding blank samples were subtracted from the aerosol and seawater samples using Xcalibur 4.2.1 software. Subsequently, MFAssignR was run in R version 4.3.2 for molecular formula assignment and data analysis. The recently developed MFAssignR is specifically designed for off-target analysis of ultra-high-resolution mass spectrometry data in complex environments and biological mixtures (Schum et al., 2020; Radoman et al., 2022). The LTQ-Orbitrap mass spectra in the m/z 150-1000 were pre-processed sequentially using the "KMDNoise" function, isotope ion filters, and internal mass recalibration before molecular formula assignment. Molecular formula assignments are limited by several conditions: signal/noise ≥ 5, $0 \le N \le 3$, $0 \le S \le 1$, $0.3 \le H/C \le 2+2/n$, $0 \le O/C \le 1$, $-10 \le DBE\text{-}O \le 10$, and error tolerance for formula assignment ≤ 3 ppm. Parameters such as double bond equivalents (DBE), aromaticity index (AI), nominal oxidation state of carbon (NOSC), and Kendrick mass defect (KMD) were used to characterize the molecular formulas in different samples.

Calculation equations of DBE (double bond equivalent), AI (aromaticity index) and NOSC (nominal oxidation state of carbon) according to the molecular elemental formula ($C_cH_hO_oN_nS_s$) assignments could be expressed as (Suo et al., 2024):

$$DBE=1+(2c-h+n)/2$$

$$AI=(1+c-o/2-h/2-s)/(c-o/2-n-s)$$

$$NOSC=4-(4c+h-3n-2o-2s)/c$$

Note that NOSC is calculated assuming that all elements are in their initial oxidation states (H = +1, O = -2, N = -3 and S = -2).

The Kendrick mass (KM) and KMD of CH2 can be directly output by MFassignR, which is calculated by the following equations:

$$KM=IUPAC\ mass\times(14/14.01565)$$

KMD=absolute (nominal KM-exact KM)

The intensity-weighted average values of C, H, N, O, S, m/z, O/C, H/C, AI, NOSC, DBE and KMD for each sample could be calculated by the following equation:

$$M_w = \sum (I_i \times M_i) / \sum_i I_i$$

where M represents parameters C, H, N, O, S, m/z, O/C, H/C, AI, NOSC, DBE and KMD, respectively; w notes an intensity-weighted average calculation, and I_i and M_i refer to the intensity and M value of peak i, respectively.

Figure S1. Triggered the phytoplankton bloom under natural sunlight. Mesocosm experiments of phytoplankton bloom were conducted by adding 4-fold diluted Guillard's F medium in 30 transparent plastic containers.

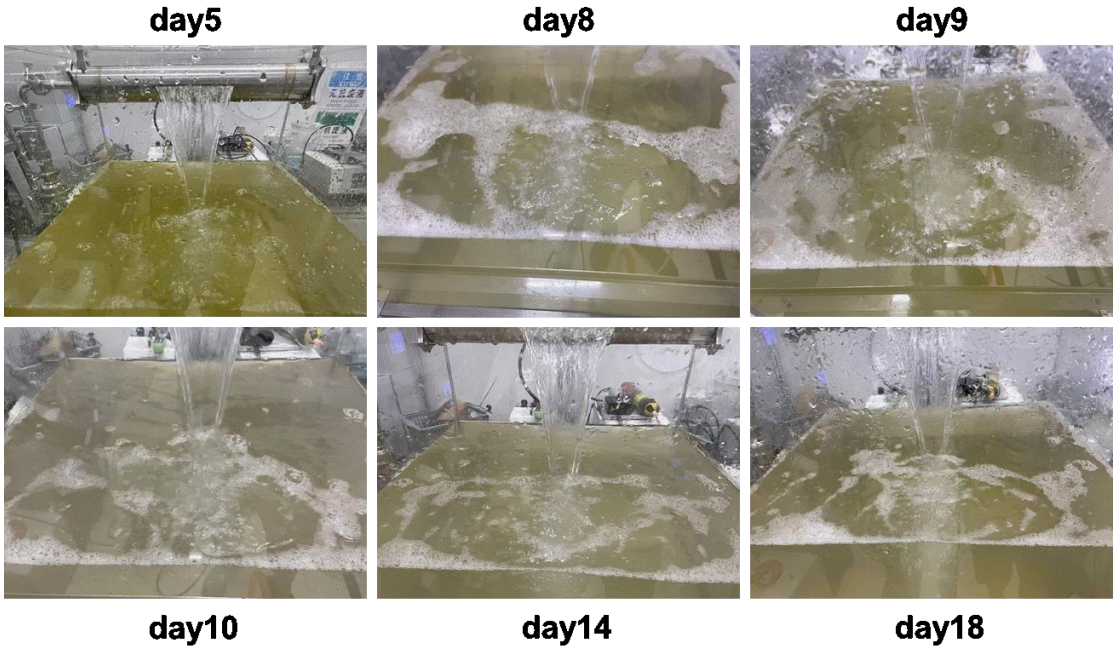

Figure S2. Bubble bursting at the surface of seawater in nascent SSA experiments. Surface bubble bursting is closely related to the surface physical properties of seawater including surface tension and viscosity. Phytoplankton blooms can significantly affect the bubble bursting process as well as the formation of SSA.

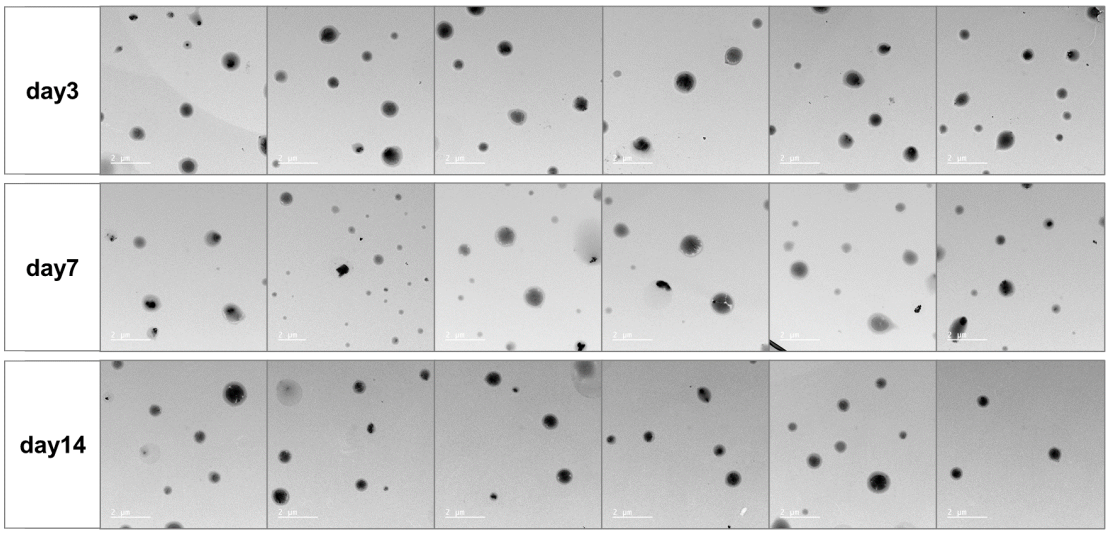

Figure S3. Transmission electron microscopy images of SSA. The sea salt core shows a black and regular shape, while the organic matter presents a gray shell encasing the sea salt core (Hu et al., 2024).

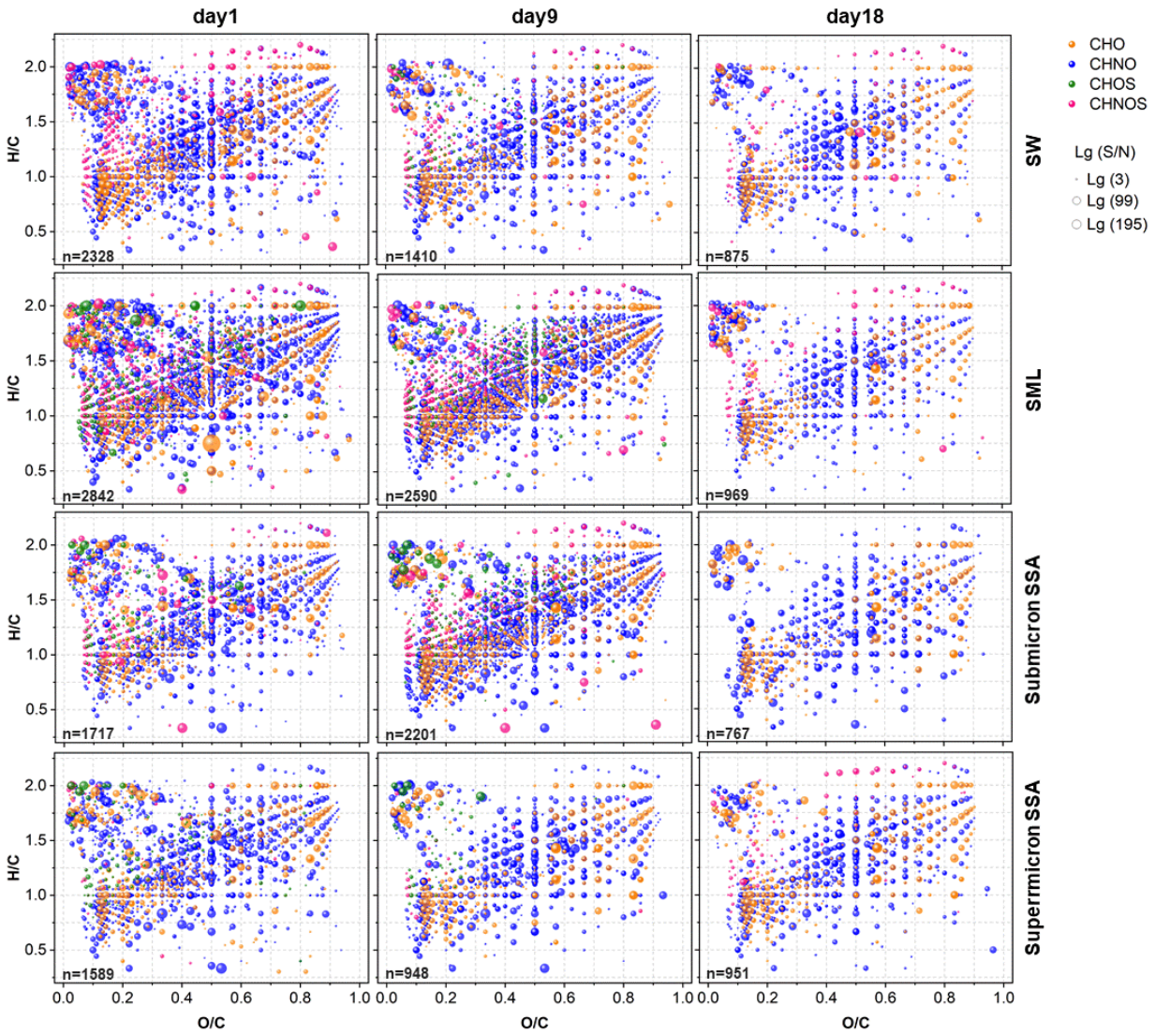

Figure S4. Sea-air transfer of organic molecules. Van Krevelen diagrams of assigned molecular formulas from different samples at the beginning, peak, and end of the phytoplankton bloom. Yellow represents CHO, blue represents CHNO, green represents CHOS, and pink represents CHNOS. To minimize the background noise in the samples, the scattered size is represented as Lg(signal/KMDnoise).

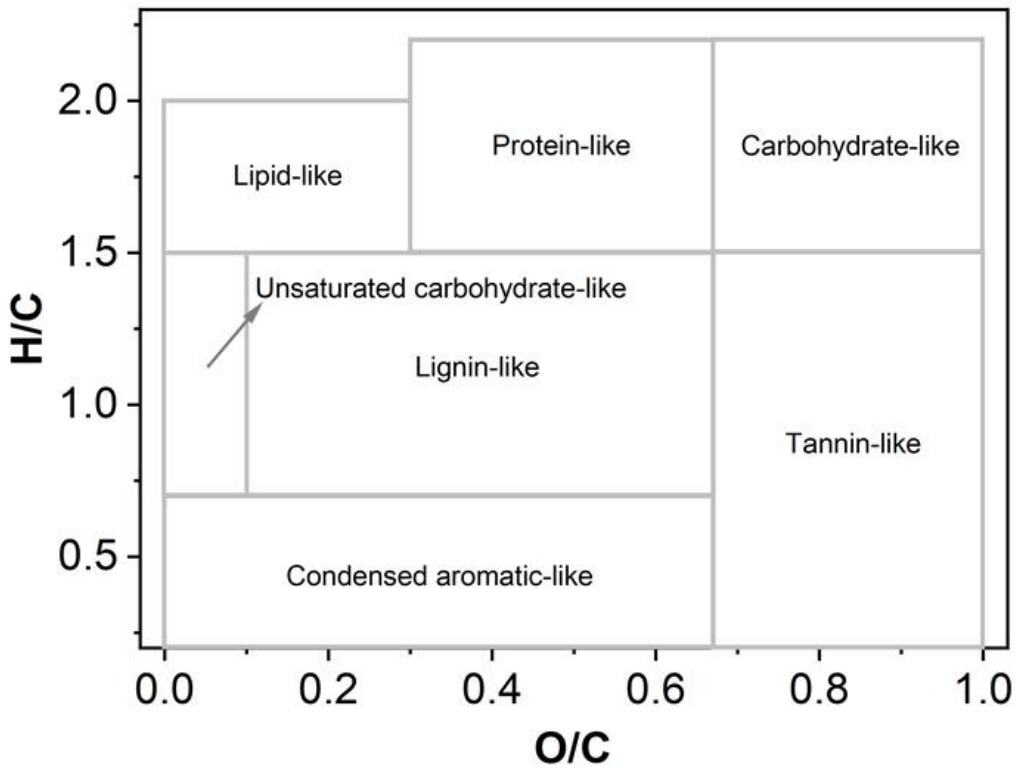

Figure S5. Chemical class regions in van Krevelen diagram space. Lipid-like ($0 < O/C \leq 0.3$; $1.5 < H/C \leq 2.0$), protein-like ($0.3 < O/C \leq 0.67$; $1.5 < H/C \leq 2.2$), carbohydrate-like ($0.67 < O/C \leq 1.2$; $1.5 < H/C \leq 2.2$), unsaturated hydrocarbon-like ($0 < O/C \leq 0.1$; $0.7 < H/C \leq 1.5$), lignin-like ($0.1 < O/C \leq 0.67$; $0.7 < H/C \leq 1.5$), tannin-like ($0.67 < O/C \leq 1.2$; $0 < H/C \leq 1.5$) and condensed aromatic-like ($0 < O/C \leq 0.67$; $0.2 < H/C \leq 0.7$) (Suo et al., 2024).

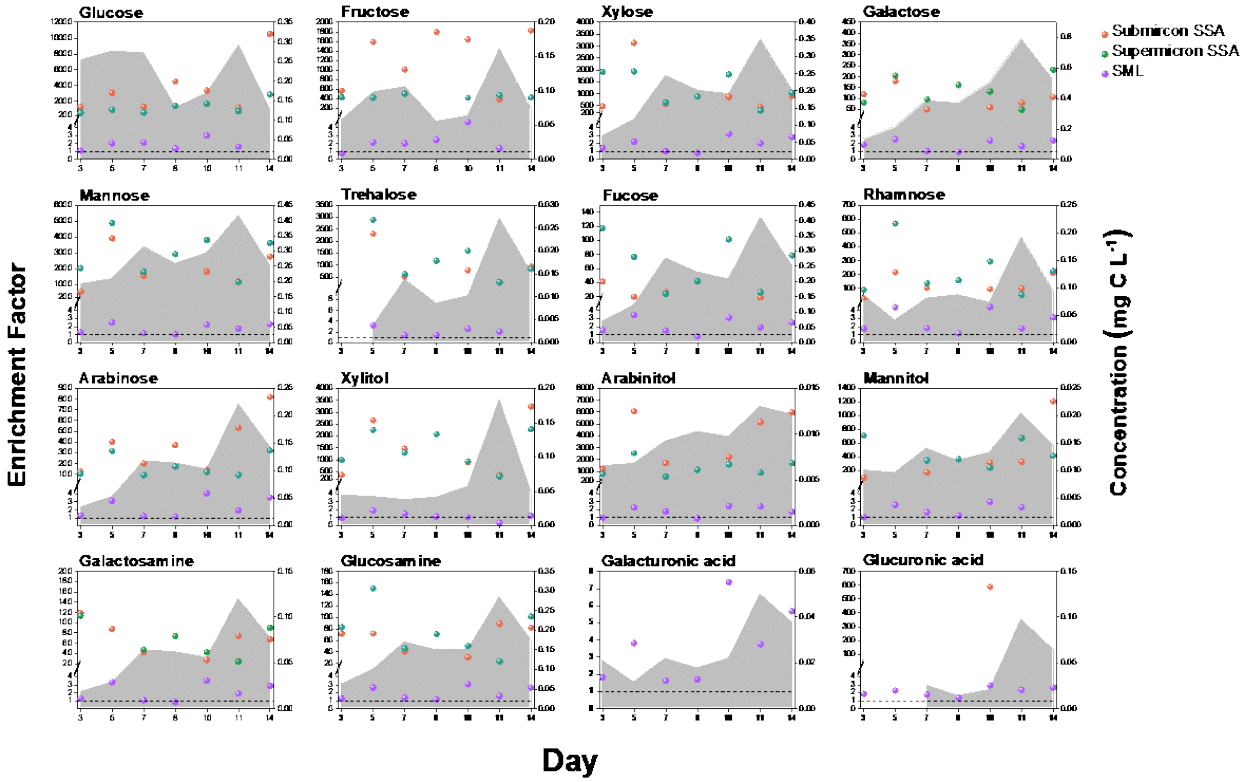

Figure S6. Fluctuations in enrichment factors of saccharides. Variation of saccharides concentration in seawater (gray shading) and their enrichment factors in SML (purple scattered points), submicron SSA (green scattered points) and supermicron SSA (orange scattered points).

Table S1. Parameter comparisons between the home-made SSA simulation tank and the Marine Aerosol Reference Tank

Parameter	home-made SSA simulation tank	Marine Aerosol Reference Tank
Volume of Tank	180 L	210 L
Material	plexiglass	plexiglass
Material of overflow pipe	stainless steels	plexiglass
Diameter of overflow pipe	9 cm	8 cm
Internal diffuser	existence	existence
Slot size	6 mm wide × 20 cm long	6 mm wide × 20 cm long
Slot to water surface	20 cm	10 cm
Seawater circulation flow	20 L min^{-1}	15 – 70 L min^{-1}
Running mode	continuous	intermittent or continuous

Table S2. Particle size classification of the low-pressure cascade impactor.

Stage	d_{50} (μm)	Stage	d_{50} (μm)
14	10	7	0.38
13	5.34	6	0.25
12	3.63	5	0.15
11	2.46	4	0.094
10	1.62	3	0.054
9	0.94	2	0.030
8	0.60	1	0.016

Table S3. Gradient elution conditions for HPAEC-PAD(Engel and Händel, 2011).

Retention time (min)	NaOH (mM)	NaAc (mM)
0	22	0
20	22	0
21	100	0
25	100	200
35	100	200
40	75	0
45	75	0
46	22	0
55	22	0
65	22	0

Table S4. Gradient elution conditions for UHPLC (Wan et al., 2022).

Retention time (min)	Mobile phase A (%)	Mobile phase B (%)
0	95	5
4	95	5
36	0	100
41	0	100
43	95	5
60	95	5

Table S5. Molecular characterization of DOC in different samples at the early (D1), peak (D9), and late (D18) stages of the phytoplankton bloom.

Samples	C_w	H_w	O_w	N_w	S_w	m/z_w	DBE_w	KMD_w	O/C_w	H/C_w	AI_w	$NOSC_w$
6/01_SW	18.437	27.283	5.465	1.377	0.079	356.949	6.484	0.218	0.398	1.346	0.327	-0.162
6/01_SML	18.657	27.584	5.604	0.914	0.095	356.130	6.327	0.217	0.420	1.218	0.388	-0.159
6/01_Submicron	19.260	29.319	6.107	1.417	0.123	381.135	6.309	0.234	0.408	1.408	0.280	-0.194
6/01_Supermicron	21.424	33.675	6.186	1.421	0.050	410.472	6.297	0.231	0.386	1.422	0.305	-0.265
6/09_SW	19.884	31.710	4.526	1.328	0.068	362.728	5.693	0.185	0.368	1.412	0.305	-0.311
6/09_SML	18.514	28.560	4.846	1.468	0.134	352.282	5.968	0.201	0.386	1.400	0.297	-0.218
6/09_Submicron	19.712	30.063	5.459	1.411	0.138	377.317	6.386	0.221	0.388	1.373	0.326	-0.199
6/09_Supermicron	17.533	27.719	4.466	1.436	0.063	330.178	5.392	0.218	0.391	1.383	0.294	-0.089
6/18_SW	17.574	26.318	5.202	1.266	0.045	338.785	6.048	0.203	0.400	1.367	0.295	-0.218
6/18_SML	20.67	30.905	4.239	1.314	0.057	368.231	5.875	0.180	0.347	1.381	0.273	-0.398
6/18_Submicron	17.256	27.130	4.081	1.461	0.099	319.133	5.421	0.168	0.397	1.361	0.386	-0.126
6/18_Supermicron	14.395	21.088	4.241	1.351	0.033	280.799	5.526	0.174	0.411	1.348	0.355	-0.079

References

Engel, A. and Händel, N.: A novel protocol for determining the concentration and composition of sugars in particulate and in high molecular weight dissolved organic matter (HMW-DOM) in seawater, Mar. Chem., 127, 180-191, https://doi.org/10.1016/j.marchem.2011.09.004, 2011.

Hu, J., Li, J., Tsona Tchinda, N., Song, Y., Xu, M., Li, K., and Du, L.: Underestimated role of sea surface temperature in sea spray aerosol formation and climate effects, npj Clim. Atmos. Sci., 7, 273, https://doi.org/10.1038/s41612-024-00823-x, 2024.

Radoman, N., Christiansen, S., Johansson, J. H., Hawkes, J. A., Bilde, M., Cousins, I. T., and Salter, M. E.: Probing the impact of a phytoplankton bloom on the chemistry of nascent sea spray aerosol using high-resolution mass spectrometry, Environ. Sci.: Atmos., 2, 1152-1169, https://doi.org/10.1039/D2EA00028H, 2022.

Schum, S. K., Brown, L. E., and Mazzoleni, L. R.: MFAssignR: Molecular formula assignment software for ultrahigh resolution mass spectrometry analysis of environmental complex mixtures, Environ. Res., 191, 110114, https://doi.org/10.1016/j.envres.2020.110114, 2020.

Suo, C., Zhao, W., Liu, S., Ren, Y., Zhang, Y., Qiu, Y., and Wu, F.: Molecular insight into algae-derived dissolved organic matters via Fourier-transform ion cyclotron resonance mass spectrometry: Effects of pretreatment methods and electrospray ionization modes, J. Hazard. Mater., 480, 136220, https://doi.org/10.1016/j.jhazmat.2024.136220, 2024.

Wan, Y., Xing, C., Wang, X., Yang, Z., Huang, X., Ge, X., Du, L., Wang, Q., and Yu, H.: Nontarget Tandem High-Resolution Mass Spectrometry Analysis of Functionalized Organic Compounds in Atmospherically Relevant Samples, Environ. Sci. Technol. Lett., 9, 1022-1029, 10.1021/acs.estlett.2c00788, 2022.